Journal of Luminescence 177 (2016) 354–360

Contents lists available at ScienceDirect

Journal of Luminescence

journal homepage: www.elsevier.com/locate/jlumin

Full Length Article

Dependence of the optical properties of Mn^{4+} activated $A_2Ge_4O_9$ (A=K,Rb) on temperature and chemical environment

Florian Baur *, Thomas Jüstel *

Department of Chemical Engineering, Münster University of Applied Sciences, Stegerwaldstrasse 39, 48565 Steinfurt, Germany

ARTICLE INFO

Article history:
Received 11 January 2016
Accepted 21 April 2016
Available online 27 April 2016

Keywords:
Racah parameters
Crystal-field splitting
Thermal quenching
Decay measurements
Red emitting Mn^{4+} phosphors

ABSTRACT

The optical properties of the novel red-emitting $K_2Ge_4O_9:Mn^{4+}$ and $Rb_2Ge_4O_9:Mn^{4+}$ phosphors exhibit an unusually strong dependence on temperature. The temperature dependence of Racah parameters *B* and *C* as well as crystal field factor Dq was determined. It was found that *C* exhibits an inverse trend in regard to *B*. This observation was linked to a potential change in bond angles of the Mn^{4+} dopant site. Mn^{4+} occupies two sites in the material, causing a double Fermi–Dirac quenching behavior. Mn^{4+} on the site with larger Mn–O distances shows a lower thermal quenching temperature. Decay constants were calculated from temperature dependent decay measurements. The constants decrease steadily with temperature, most likely not due to thermal quenching but an increase of the $^2E \rightarrow {}^4A_2$ transition probability.

1. Introduction

Solid-state lighting, especially based on phosphor converted light emitting diodes (pcLEDs), is gaining ever increasing importance [1–3]. For domestic application warm-white light, resembling that of incandescent light sources, is generally considered the most suitable [4]. In an eligible host material the excitation and emission spectrum of Mn^{4+} is a close match for the ideal red emitter for the generation of warm-white light by conversion of blue 450 nm emission [5]. Accordingly, research activity and commercial focus on the Mn^{4+} ion is high [6–15]. The newly discovered $A_2Ge_4O_9:Mn^{4+}$ phosphors described in this work were patented in 2014 [16]. It is well known that the optical properties of Mn^{4+} strongly depend on the chemical environment of the activator ion. Emission wavelengths ranging from 620 nm to 720 nm have been reported [17,18]. A low wavelength of the emission band is crucial in obtaining high efficiency pcLEDs. Emission in the deep red region, as observed in the commercial $Mg_{14}Ge_5O_{24}:Mn^{4+}$ phosphor, yields mediocre luminous efficacy (LE) and color rendering index (CRI) [19]. Contrary to that, the Mn^{4+} activated hexafluorides, firstly reported by Paulusz in 1973, were shown to exhibit excellent LE and CRI by Setlur et al. in 2010 [17,20]. Accordingly, being able to approximate the emission wavelength of Mn^{4+} in a specific host material is crucial for an efficient research for Mn^{4+}-based pcLED phosphors. While the influence of the crystal field parameter Dq and the Racah parameters *B* and *C* is well understood, so far it is not possible to predict their values from the host material's properties. However, recent publications by Brik and Srivastava report progress in that direction [10,14,21]. The red-emitting alkali germanates described in this work can yield additional insight into the host-activator interaction of Mn^{4+}.

2. Experimental section

Samples of $K_2(Ge_{0.999}Mn_{0.001})_4O_9$ and $Rb_2(Ge_{0.999}Mn_{0.001})_4O_9$ were prepared by conventional solid state reaction. Stoichiometric amounts of K_2CO_3 (99.0%, AlfaAesar) or Rb_2CO_3 (99.0%, AlfaAesar), respectively, GeO_2 (99.999%, AlfaAesar) and $MnC_2O_4 \cdot 2H_2O$ (99.0%, Dr. Paul Lohmann) were thoroughly mixed in an agate mortar in acetone. The resulting mixtures were dried, transferred to porcelain crucibles and calcined at 600 °C for 2 h in air. After calcination the powders were reground, and 10 mol% excess KF (99%, Merck) or Rb_2CO_3 (99%, Alfa Aesar), respectively, were added as a flux and as compensation for a loss of the volatile alkali metal ions. The resulting mixtures were annealed at 800 °C for 4 h and afterwards washed in H_2O to remove water-soluble impurities.

XRD, fluorescence, reflection and decay measurements and calculation of external quantum efficiency (EQE) were performed as published earlier [22]. Additional wavelength correction was performed against an Hg lamp on the day of the measurement.

* Corresponding authors. Tel.: +49 2551962205.
E-mail addresses: florian.baur@fh-muenster.de (F. Baur), tj@fh-muenster.de (T. Jüstel).

http://dx.doi.org/10.1016/j.jlumin.2016.04.046
0022-2313/

Each spectrum was recorded five times, accumulating the data to minimize noise. Integration time per step was set to 0.4 s.

Temperature dependent reflection spectra and the emission spectra for temperature dependent quantum efficiency measurements were obtained using a barium sulfate coated alumina integration sphere. The sphere was equipped with a heating element controlled by an EUC943 PID-controller manufactured by Enda company.

3. Results and discussion

$K_2Ge_4O_9$ and $Rb_2Ge_4O_9$ are isostructural and crystallize in the trigonal space group $P\bar{3}c1$ (158) [23–26]. The structure has been redetermined and refined several times. The latest publication is that of Redhammer and Tippelt in 2013 who described the structure as follows. The dominant building unit are isolated three-membered Ge_3O_9 rings forming layers within the *ab* plane. The rings comprise two tetrahedrally coordinated Ge-sites, Ge(2) and Ge(3). The layers are connected by two crystallographically different GeO_6 octahedra (Ge(1) and Ge(4)). The Ge(1)O_6 octahedra have site symmetry $\bar{3}$, while the Ge(4)O_6 octahedra are less regular with site symmetry 3. Both octahedra show higher regularity in the Rb-compound. The Ge1–O distances are larger than the Ge4–O distances. Structural data as published by Redhammer and Tippelt is listed in Table 1. According to Vegard's law a solid solution series $(Rb_{1-x}K_x)_2Ge_4O_9$ with $0 \leq x \leq 1$ should exist. Several samples with varying *x* were prepared and derived host lattice parameters show the formation of a solid solution in each sample.

Due to its [Ar]$3d^3$ configuration, Mn^{4+} strongly prefers octahedrally coordinated sites as the crystal field stabilization energy will be maximized. No visible emission has been observed from materials with tetrahedrally coordinated Mn^{4+} ions [27]. Therefore, it can be concluded that Mn^{4+} will occupy the octahedrally coordinated Ge(1) and Ge(4) sites.

The XRD patterns as depicted in Fig. 1 reveal the formation of the target phase. A minor impurity can be observed in the $Rb_2(Ge_{0.999}Mn_{0.001})_4O_9$ pattern as reflexes at 28.4° and 28.7° appear unknown for the target phase. They match the main reflexes of cristobalite- and rutile-type GeO_2 [28,29], respectively, and are most likely caused by unreacted educt.

Reflectance spectra recorded between 300 K and 450 K are depicted in Fig. 2. The low-energy shoulder of the broad absorption band is assigned to the spin-allowed $^4A_2$ to $^4T_2$ transition of Mn^{4+}. For d^3 ions the energy of the $^4T_2$ level relative to the ground state is equal to 10 Dq. A red-shift of the band with increasing temperature can be observed in both spectra. The broad

Table 1
Lattice parameters, selected bond lengths, angles and site symmetries of $K_2Ge_4O_9$ and $Rb_2Ge_4O_9$ as published by Redhammer and Tippelt [26].

	$K_2Ge_4O_9$	$Rb_2Ge_4O_9$
a/nm	1.18461	1.21008
b/nm	0.98009	0.98722
Ge1 octahedron		
< Ge–O > /pm	190.8	190.7
Angle axial–axial	180.00°	180.00°
Site symmetry	3	3
Ge4 octahedron		
< Ge–O3 >	188.6	189.1
< Ge–O4 >	186.5	187.0
Angle axial–axial	178.18°	178.58°
Site symmetry	3	3

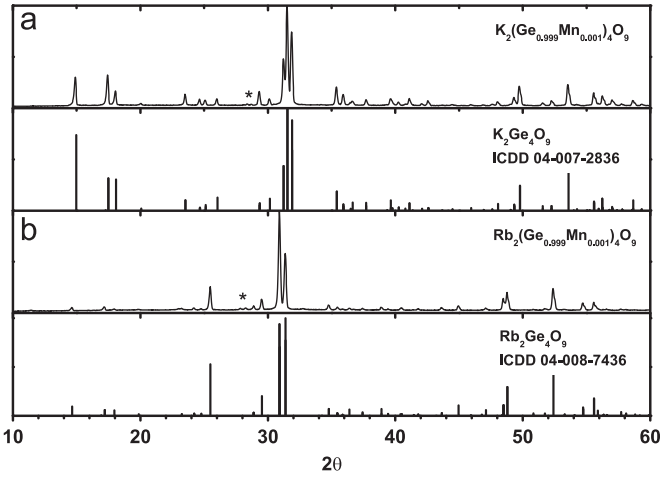

Fig. 1. XRD patterns of the synthesized (a) $K_2(Ge_{0.999}Mn_{0.001})_4O_9$ and (b) $Rb_2(Ge_{0.999}Mn_{0.001})_4O_9$ powders with their respective ICDD references.

absorption band in the UV range mainly consists of an O^{2-} to Mn^{4+} ligand-to-metal charge transfer (LMCT) band and the spin-allowed $^4A_2$ to $^4T_1$ band. The spin-forbidden $^4A_2$ to $^2T_2$ band, energetically located between the two spin-allowed bands, cannot be distinguished due to its weak intensity. With increasing temperature the shape of the reflectance spectra changes. This indicates changes of the positions of the underlying absorption bands. For further elucidation, excitation spectra were recorded at temperatures from 77 K to 500 K (Fig. 3). A broad and structured excitation band can be observed in the range of 18,000 cm^{-1} to 40,000 cm^{-1} for both samples. The peaks around 22,000 and 21,000 cm^{-1} (455 nm and 475 nm), respectively, arise from the $^4A_2$ to $^4T_2$ transitions. The crystal field splitting (CFS) is stronger in $K_2(Ge_{0.999}Mn_{0.001})_4O_9$, agreeing with the smaller Mn–O distance in this material. The prominent peak's position at 33,000 cm^{-1} (300 nm) is similar in both materials and is relatively independent of the temperature. 2*p* to 3*d* LMCT transitions are allowed and therefore of high intensity, furthermore, their energy does not strongly depend on the ligand-to-metal distance, i.e. the temperature. Therefore, the 33,000 cm^{-1} peak is assigned to the O^{2-} to Mn^{4+} LMCT. The relative intensity of the LMCT band is stronger in $K_2(Ge_{0.999}Mn_{0.001})_4O_9$. This is likely caused by the larger size of the Rb cation resulting in a lower quantum efficiency of the transition. The peaks around 30,000 cm^{-1} (330 nm) are attributed to the $^4A_2$ to $^4T_1$ transitions of the two materials. Located between the $^4T_1$ and $^4T_2$ bands at 26,000 cm^{-1} (390 nm) is a minor peak arising from the spin-forbidden $^4A_2$ to $^2T_2$ transition [7,30]. At 21,551 cm^{-1} (464 nm) The energy position of the $^4T_1$ level correlates with both Dq and Racah parameter *B*. From the reflectance spectra it can be assumed that Dq decreases with increasing temperature in $A_2Ge_4O_9$:Mn^{4+}. The strength of the CFS is strongly influenced by the distance between the ligands and the central ion. In the literature, an approximate relation of

$$\mathrm{CFS} = K/R^n \quad (1)$$

where *K* is a constant, *R* is the ligand-metal distance and *n* is a proportionality factor, is found for octahedrally coordinated transition metals. For 3*d* ions, i.e. Mn^{4+}, $n \approx 5$ [21,31,32]. The expected expansion of the host matrix with increasing temperature explains the observed red-shifts.

Throughout the measured temperature range the Rb-sample exhibits a lower CFS than the Potassium comprising sample. This can be expected due to the larger size of the Ge-sites. From Eq. (1)

$$\frac{Dq_{Rb}}{Dq_K} = \left(\frac{R_K}{R_{Rb}}\right)^n \quad (2)$$